8. THE OXYGEN ISOTOPIC COMPOSITION OF INTERSTITIAL WATERS: EVIDENCE FOR FLUID FLOW AND RECRYSTALLIZATION IN THE MARGIN OF THE GREAT BAHAMA BANK[1]

Peter K. Swart[2]

ABSTRACT

This study investigates the $\delta^{18}O$ of pore waters from Sites 1003 through 1007, drilled along the western margin of the Great Bahama Bank during Leg 166 of the Ocean Drilling Program. These pore waters generally show a positive correlation between $\delta^{18}O$ and the concentration of chloride. The exception to this trend is Site 1006, where the pore waters exhibit nonlinear behavior with respect to chloride. The correlation between the concentration of Cl^- and $\delta^{18}O$ at most of the sites appears to be a coincidence because although the increase in Cl^- is a result of diffusion from an underlying source, the increases in $\delta^{18}O$ result from the recrystallization of metastable carbonates in the presence of a geothermal gradient. The difference in behavior in the $\delta^{18}O$ of the pore water at Site 1006 is probably a result of the relative reduced rate of carbonate recrystallization at this site. The $\delta^{18}O$ of the pore waters in the upper portion of the cores shows a pattern similar to the concentration of chloride in that there is an interval of 30–50 m in which neither the $\delta^{18}O$ nor the concentration of Cl^- changes. This interval is consistent with either an interval of very rapid deposition of sediment or the advection of fluid through the platform. Both the $\delta^{18}O$ and the concentration of Cl^- increase toward the platform, suggesting an input of saline and isotopically heavy water from the platform surface.

INTRODUCTION

During Leg 166 of the Ocean Drilling Program (ODP), scientists drilled a transect of sites along the extension of the Western Geophysical Seismic Line (Fig. 1) into the Straits of Florida to examine the development of the margin of the Great Bahama Bank and to examine potential fluid flow through a carbonate platform (Eberli, Swart, Malone, et al., 1997; Shipboard Scientific Party, 1997). The sediments at these sites, late Oligocene to Holocene in age, were principally composed of material derived from three sources: (1) aragonite and high-magnesium calcite from the Great Bahama Bank, (2) pelagically derived low-magnesium calcite and aragonite, and (3) sediments derived from the weathering of Cuba and Hispaniola. Variations in the contributions from these three sources were controlled by changes in sea level, with banktop-derived sediments dominating during highstands and pelagic and siliciclastic materials becoming more important during lowstands (Eberli, Swart, Malone, et al., 1997). The sites closest to the margin of the Great Bahama Bank—Sites 1005, 1004, and 1003—were more influenced by carbonate production on the platform top showing high rates of accumulation during highstands and reduced or little sedimentation during sea-level lowstands. Rates of deposition at Sites 1003 through 1005 were ~100 m/m.y. over the upper 100 m. Below this depth, rates declined (Shipboard Scientific Party, 1997). Rates of deposition were slightly reduced at Sites 1006 and 1007 in the upper 50 to 100 meters below seafloor (mbsf). Details of the sedimentology and rates of deposition were provide by Eberli, Swart, Malone, et al. (1997) and Shipboard Scientific Party (1997).

During the drilling of these sites, geochemical measurements on interstitial water samples revealed the presence of a zone in which there was an absence of changes in the concentrations of both conservative and nonconservative minor and trace element constituents in the pore waters (Shipboard Scientific Party, 1997). Although less convincing, similar trends were noted in the temperature profiles measured using the Adara and water-sampling temperature probe

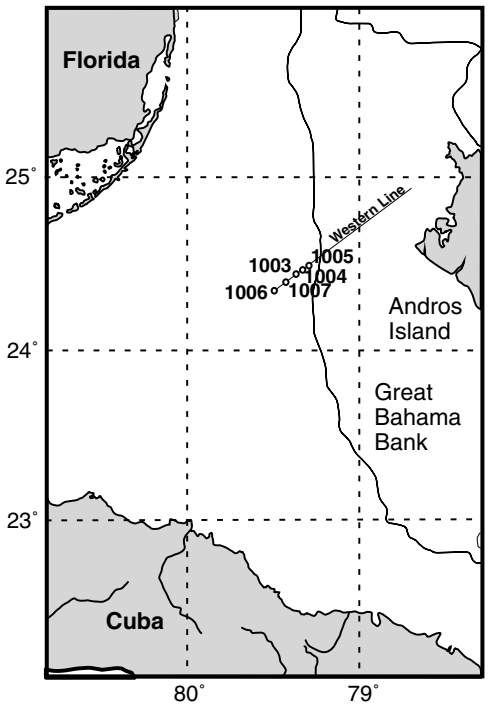

Figure 1. Location map showing the approximate positions of Sites 1003–1007 on the western margin of the Great Bahama Bank. In order of distance from the platform margin, the sites are 1005, 1004, 1003, 1007, and 1006.

temperature tools (Eberli, Swart, Malone, et al., 1997). The isochemical trends are well illustrated if the concentrations of chloride (Fig. 2A) and strontium (Fig. 2B) in the pore waters in the upper 100 mbsf are examined. Both these elements exhibit a region with no changes in the concentrations, overlying a zone in which there is a rapid increase in concentration. In the case of chloride, the high concentration at depth appears to be related to diffusion from an underlying chloride-rich source such as evaporated seawater or an evaporite deposit, like that encountered previously in the Bahamas (Austin,

[1]Swart, P.K., Eberli, G.P., Malone, M.J., and Sarg, J.F. (Eds.), 2000. *Proc. ODP, Sci. Results,* 166: College Station TX (Ocean Drilling Program).

[2]Division of Marine Geology and Geophysics, University of Miami, 4600 Rickenbacker Causeway, Miami FL 33149, USA. pswart@rsmas.miami.edu

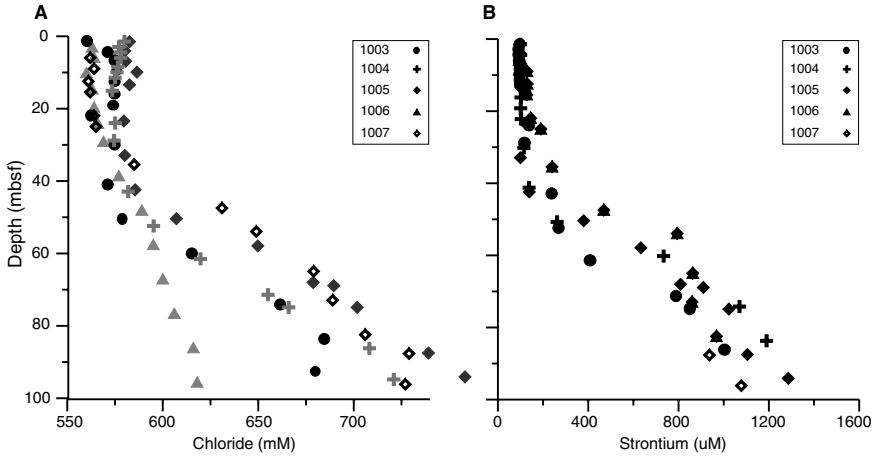

Figure 2. **A.** Concentration of chloride in the pore waters in the upper 100 mbsf (the flushed zone), Sites 1003–1007. **B.** Concentration of pore-water strontium in the upper 100 mbsf (the flushed zone), Sites 1003–1007. Data are from Eberli, Swart, Malone, et al. (1997).

Schlager, et al., 1986). This upper zone has been termed the flushed zone. Below the flushed zone, there are rapid changes in all of the conservative and nonconservative constituents. Changes in the nonconservative components such as Sr^{2+}, Ca^{2+}, and Mg^{2+} are related to the recrystallization of metastable carbonates (Baker et al., 1982; Swart and Guzikowski, 1988). Changes in the SO_4^{2-} and alkalinity are related to the oxidation of organic material. In addition to the upper flushed zone, there is a region near the platform margin at Sites 1004 and 1005 where the chloride concentration suggests that normal marine water is being drawn into the platform, presumably by some type of convection mechanism (Fig. 3). The purpose of this paper is to present data on the $\delta^{18}O$ of pore waters to (1) further constrain the origin of waters in the flushed zone, (2) examine the origin of the increase in chloride concentration with depth, and (3) examine the apparent chloride anomaly near the platform margin and ascertain whether it is a result of bottom water being advected into the platform.

TECHNIQUES

Interstitial water samples were obtained using conventional methods (Manheim and Sayles, 1974). Chloride concentrations were measured on the ship (Eberli, Swart, Malone, et al., 1997) using methods described by Gieskes (1973, 1974). Oxygen and hydrogen isotopic measurements of the pore waters were made in the Division of Marine Geology and Geophysics at the University of Miami. Hydrogen isotopic data were only analyzed on one hole as a result of operational problems. Oxygen isotopic data were made in duplicate on most samples from Sites 1003 through 1007. As the methods for the measurement of both isotopes are different from the conventional techniques (Epstein and Mayeda, 1953; Friedman, 1957), they will be elaborated here. Both measurements were made using a water equilibration system (WEST) attached to a Europa GEO. In the WEST, the oxygen isotopic composition is determined on CO_2 that has been injected into serum bottles at slightly above atmospheric pressure containing 1 cm^3 of sample. The samples are subsequently equilibrated at 40°C for 4 hr without shaking. The process is entirely automated: the CO_2 is injected into the sample bottles and retrieved using an autosampler, and the gas is transferred to a dual-inlet mass spectrometer through a cryogenic trap (–70°C) to remove water. The precision of this method for oxygen, determined by measuring 59 samples of our internal standard, is ±0.07‰ (Fig. 4). The relatively large standard deviation is a result of a 0.3°C temperature variation in the equilibration bath. The hydrogen isotopic composition is determined using the same device as employed for CO_2. Equilibration with hydrogen gas takes place in the presence of a platinum catalyst (Hokko Beads) at 40°C (Coplen et al., 1991). As a result of the above-mentioned stability problems with the temperature bath, precision using this method is ±1.5‰ (Fig. 4). All data are calibrated using Vienna Standard Mean Ocean Water (SMOW) and are reported in parts per thousand (‰) according to the conventional notation.

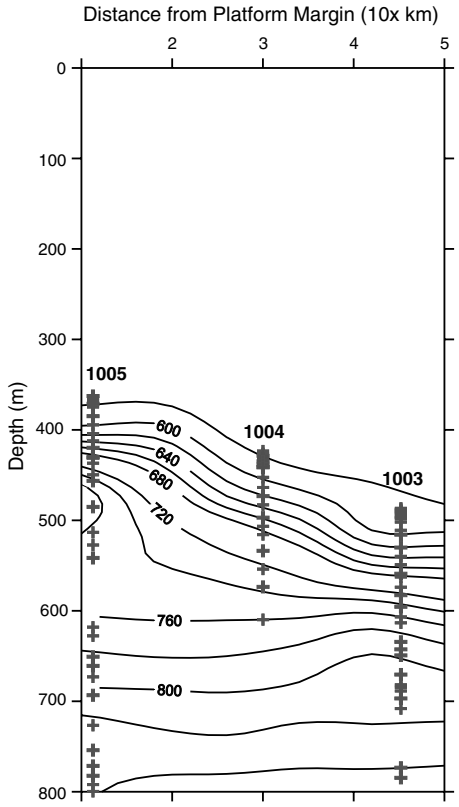

Figure 3. Contour map of chloride for the three sites closest to the platform. Location of sites and sampling intervals are shown (Shipboard Scientific Party, 1997).

RESULTS

The $\delta^{18}O$ data for Sites 1003 through 1007 are shown in Figure 5 and Tables 1–5. At all sites, the $\delta^{18}O$ of the pore waters in the upper flushed zone (0 to 30 mbsf) is fairly constant (1 σ = 0.05‰ to 0.08‰) (Fig. 6); sites closer to the Great Bahama Bank (Sites 1005, 1004, and 1003) are more positive in their $\delta^{18}O$ values than sites farther away (Sites 1007 and 1006) (Table 6; Fig. 7). Below the flushed zone, the $\delta^{18}O$ values of the pore waters at all sites increase sharply to more

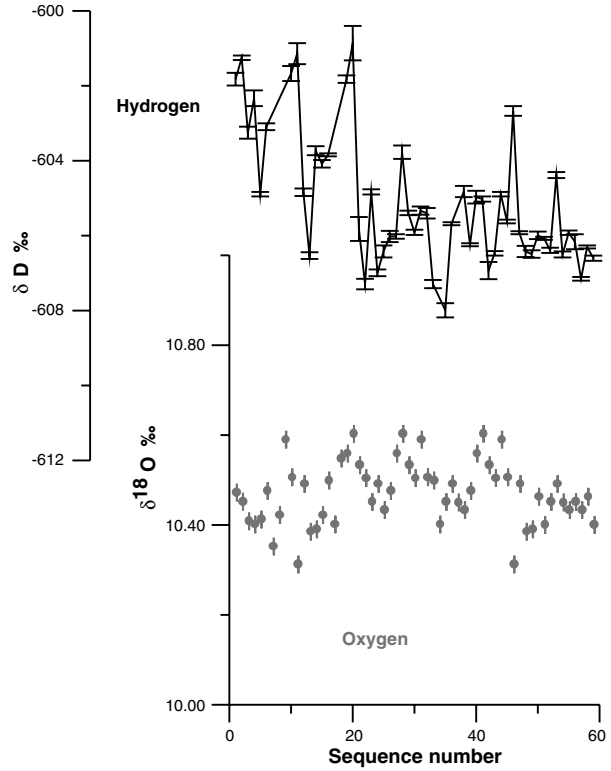

Figure 4. Results showing the reproducibility of oxygen and hydrogen equilibration. Error bars indicate ±1 standard error for analyses. The large range in the reproducibility of the hydrogen ($1\sigma = 1.5‰$) arises from the high degree of temperature sensitivity for the equilibration (Coplen et al., 1991). This temperature stability affects the $\delta^{18}O$ as well but to a much lesser extent.

than +2‰ (Figs. 4, 8) and exhibit a positive correlation with the concentration of chloride (Fig. 9). The exception to this trend occurs at Site 1006, where the $\delta^{18}O$ values increase to only around +0.8‰ before decreasing again with increasing depth (Table 5; Figs. 5, 10). The highest $\delta^{18}O$ value of +2.89‰ occurs at Site 1003 at a depth of 910.14 mbsf. The δD value was determined in selected samples from Site 1003. Although the replicate samples were not within the standard deviation of the laboratory standards, the data indicate a decrease in the δD of the pore waters in the lower portion of Site 1003 (Fig. 11).

DISCUSSION

Evidence for the Flushed Zone

The $\delta^{18}O$ values in the upper portion of the sediments in conjunction with the uniform concentration of Sr^{2+} and Cl^- (Table 6; Fig. 6) in the pore fluids support our ideas of active fluid movement in this portion of the profile (Shipboard Scientific Party, 1997). It is also possible that a period with a very high rate of sedimentation could have produced a pattern in the pore-water geochemistry similar to that observed. In order for this mechanism to be responsible, the entire thickness of the flushed zone must have been deposited over a geologically short period of time. Although this mechanism is unlikely based on the present rates of sedimentation (Shipboard Scientific Party, 1997), it is possible that rates of deposition are outside the range of the chronostratigraphic markers used in this study. Some support for this idea might be provided by the presence of a thinner flushed zone in Sites 1003 and 1007, which shows depositional rates of ~5 cm/k.y. over the upper 50 mbsf compared to 10–15 cm/k.y. at Sites 1003 through 1005.

Within the reproducibility of the replicate $\delta^{18}O$ analyses and the standard deviation of our standards, there appears to be some variation in the upper portions of the flushed zone that is not evident in the

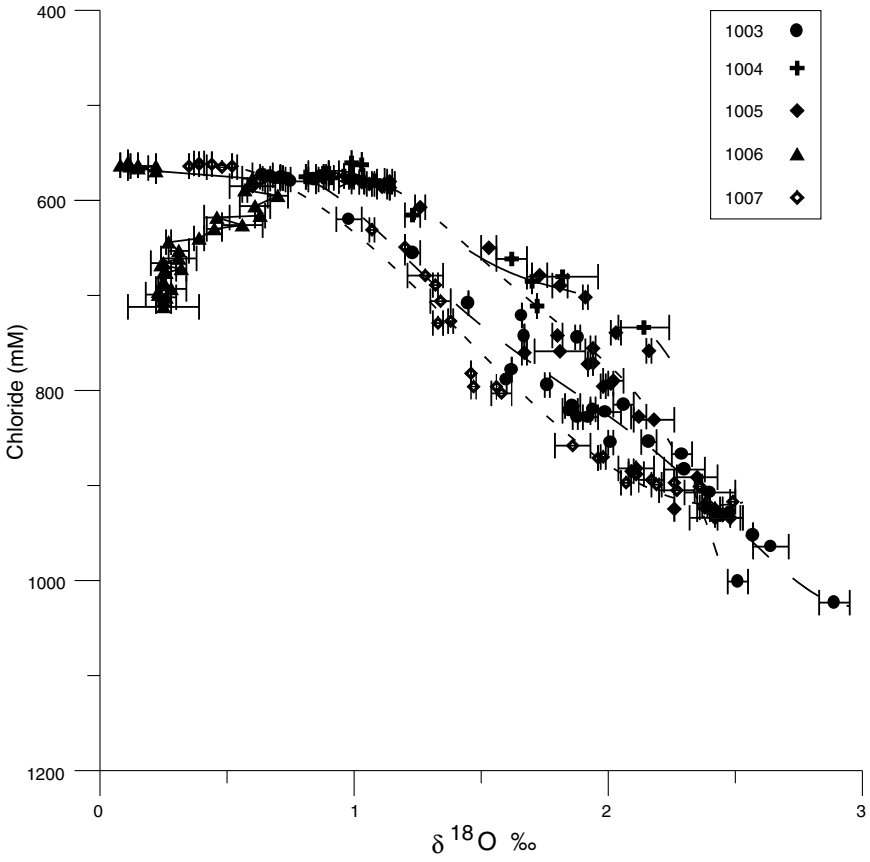

Figure 5. Chloride vs. $\delta^{18}O$ for all five sites. Note the strong degree of co-variance between the $\delta^{18}O$ and Cl^-, with the exception of Site 1006. Chloride data are from Eberli, Swart, Malone, et al. (1997). Error bars represent ±1 standard deviation.

Table 1. The oxygen and hydrogen isotopic composition of waters from Site 1003.

Core, section, interval (cm)	Depth (m)	O #1	O #2	Mean	SD
166-1003A-					
1H-1, 145-150	1.45	0.90	0.70	0.75	0.10
1H-2, 145-150	2.95	0.70	0.67	0.69	0.02
1H-3, 145-150	4.45	0.82	0.87	0.84	0.02
1H-4, 145-150	5.95	0.75	0.73	0.74	0.01
2H-1, 145-150	8.45	0.72		0.72	
2H-2, 145-150	9.95	0.71		0.71	
2H-3, 145-150	11.45	0.89	0.84	0.87	0.02
2H-6, 145-150	15.03	0.60	0.69	0.64	0.04
3H-5, 145-150	23.95	0.71	0.63	0.67	0.04
4H-2, 140-150	28.81				
5H-5, 140-150	42.90				
6H-5, 140-150	52.40				
7H-5, 140-150	61.50	1.03	0.94	0.98	0.05
8H-5, 140-150	71.40	1.26	1.20	1.23	0.03
9H-1, 140-150	74.90				
11X-1, 140-150	86.20	1.46	1.45	1.45	0.00
12X-2, 140-150	94.80	1.66	1.67	1.66	0.00
13X-4, 140-150	107.50	1.67		1.67	
14X-5, 140-150	118.50				
15X-3, 135-150	125.05	1.62		1.62	
17X-4, 135-150	145.75	1.60		1.60	
18X-3, 135-150	153.95				
19X-1, 135-150	160.55	1.76	1.77	1.76	0.01
22H-5, 135-150	195.45	1.82	1.88	1.85	0.03
20X-4, 135-150	181.45	1.83	1.89	1.86	0.03
166-1003B-					
21X-5, 135-150	192.65	1.92	1.95	1.94	0.01
22X-3, 135-150	199.35	1.86	1.90	1.88	0.02
23X-2, 135-150	207.55	1.88	1.97	1.92	0.04
24X-3, 135-150	218.65	1.93	2.06	1.99	0.06
31X-1, 135-150	283.15	2.01	2.10	2.06	0.04
32X-2, 135-150	294.25	2.13	2.20	2.16	0.03
35X-1, 135-150	321.55	2.24	2.33	2.29	0.04
36X-2, 135-150	332.75	2.01	2.02	2.01	0.01
39X-1, 100-117	359.60	2.23	2.38	2.30	0.08
48X-CC, 5-15	446.43	2.48	2.48	2.48	0.00
49X-1, 25-40	455.15	2.30	2.49	2.40	0.10
50X-1, 135-150	465.95	2.57	2.57	2.57	0.00
54X-1, 135-150	504.45	1.87	1.89	1.88	0.01
166-1003C-					
1R-1, 40-45	506.40				
22R-3, 34-44	658.64				
25R-1, 38-42	684.88				
30R-4, 35-45	737.15				
32R-7, 0-16	759.69	2.71	2.57	2.64	0.07
34R-4, 0-19	773.58	2.55	2.46	2.51	0.04
39R-1, 120-131	820.20				
48R-4, 113-126	910.14	2.83	2.95	2.89	0.06
58R-1, 58-62	1002.38				
60R-3, 0-9	1024.08				
61R-2, 0-10	1032.15				
66R-4, 56-70	1083.59				

Note: All samples were run in replicate, and values for individual analyses, means, and standard deviations (SD) are shown.

Cl^- data. It is possible that this variability is real; alternatively, it is possible that it results from nonuniformity in the manner in which the samples were sealed. The increasing $\delta^{18}O$ of the pore waters in the flushed zone closer to the margin of the carbonate platform probably indicates that the bottom waters at these sites originated from the surface of the Great Bahama Bank—perhaps during the winter, when cold, dense saline water is known to cascade over the margin.

Origin of the Increase in Chloride with Depth

The increase in the concentration of chloride with increasing depth noted at all the sites during Leg 166 was postulated to be a result of the diffusion of Cl^- from an underlying evaporitic source (Shipboard Scientific Party, 1997). Such a source was drilled at Site 627, north of Little Bahama Bank (Austin, Schlager, et al., 1986), and pore waters showed a similar increase in Cl^- approaching this source (Swart and Guzikowski, 1988). However, analysis of the Na^+/Cl^- ratios of the interstitial pore-water data from Leg 166 reveals no evidence of a NaCl source. Perhaps a more likely origin is simply evap-

Table 2. The oxygen isotopic composition of samples from Hole 1004A.

Core, section, interval (cm)	Depth (m)	O #1	O #2	Mean	SD
166-1004A-					
1H-1, 145-150	1.45	0.99	0.99	0.99	0.00
1H-3, 145-150	4.45	0.94	0.83	0.88	0.06
2H-1, 140-150	6.70	1.00	0.99	0.99	0.01
2H-3, 140-150	9.70	0.90	0.92	0.91	0.01
2H-5, 140-150	12.70		0.88	0.88	
3H-1, 140-150	16.20		0.99	0.99	
3H-3, 140-150	19.20		0.96	0.96	
3H-5, 140-150	22.20		1.03	1.03	
4H-4, 140-150	30.20		0.81	0.81	
5H-5, 140-150	41.20		0.90	0.90	
6H-5, 140-150	50.70	1.12	1.05	1.08	0.04
7H-5, 140-150	60.20	1.20	1.26	1.23	0.03
9H-5, 140-150	74.20	1.68	1.57	1.62	0.06
10H-5, 140-150	83.70		1.70	1.70	
11H-5, 92-102	92.72	1.69	1.96	1.82	0.14
14X-2, 140-150	110.40	1.72		1.72	0.00
16X-3, 135-150	130.35				
18X-4, 89-105	149.79	2.24	2.04	2.14	0.10
22X-3, 135-150	185.55				

Note: All samples were run in replicate, and values for individual analyses, means, and standard deviations (SD) are shown.

Table 3. The oxygen isotopic composition of samples from Site 1005.

Core, section, interval (cm)	Depth (m)	O #1	O #2	Mean	SD
166-1005A-					
1H-1, 145-150	1.50	1.05	1.07	1.06	0.01
2H-1, 145-150	4.00	1.12	1.15	1.14	0.01
2H-3, 140-150	6.90	1.02	1.03	1.03	0.01
2H-5, 140-150	9.90	1.14		1.14	0.00
3H-1, 140-150	13.40	1.09	1.16	1.12	0.04
4H-5, 140-150	23.40	1.04	0.95	0.99	0.05
5H-5, 140-150	32.90	1.10	0.99	1.04	0.05
6H-5, 140-150	42.40	1.13	1.09	1.11	0.02
7H-4, 140-150	50.40	1.24	1.28	1.26	0.02
8H-4, 140-150	57.90	1.50	1.57	1.53	0.03
9H-5, 135-150	68.00	1.70	1.75	1.73	0.03
10X-1, 135-150	68.90	1.84	1.77	1.81	0.03
11X-1, 135-150	74.90	1.92	1.90	1.91	0.01
12X-4, 135-102	87.50	2.05	2.01	2.03	0.02
13X-2, 135-150	94.10	2.17	2.14	2.16	0.01
16X-2, 135-150	122.40	2.00	1.97	1.98	0.01
19X-2, 135-150	150.30	1.66	1.69	1.67	0.01
20X-5, 135-150	164.10	1.71	1.91	1.81	0.10
22X-2, 135-150	178.20	1.82	1.78	1.80	0.02
30X-3, 135-150	253.80	1.93	1.95	1.94	0.01
31X-3, 135-150	263.20	1.92		1.92	0.00
34X-2, 135-150	286.00	1.94	1.94	1.94	0.00
35X-2, 135-150	296.00	1.98	2.06	2.02	0.04
36X-2, 135-150	308.00	2.02	2.00	2.01	0.01
38X-1, 135-150	328.00				
42X-1, 135-150	360.90	2.10	2.27	2.18	0.08
166-1005C-					
1R-1, 140-150	388.00	2.15	2.10	2.12	0.03
3R-1, 0-8	405.20				
4R-2, 0-7	416.00				
5R-2, 0-8	425.50				
6R-1, 0-4	433.00				
9R-1, 0-10	460.70				
12R-2, 0-10	490.10				
16R-1, 0-10	528.30	2.43	2.27	2.35	0.08
19R-1, 0-5	553.30				
20R-2, 124-135	565.40	2.26		2.26	0.00
21R-1, 145-150	573.20				
24R-2, 50-58	601.00				
28R-1, 102-111	637.00				
33R-2, 0-11	682.50				

Note: All samples were run in replicate, and values for individual analyses, means, and standard deviations (SD) are shown.

Table 4. The oxygen isotopic composition of samples from Hole 1006A.

Core, section, interval (cm)	Depth (m)	O #1	O #2	Mean	SD
166-1006A-					
1H-2, 143-150	2.93	0.15		0.15	0.00
1H-4, 128-135	5.78	0.12		0.12	0.00
2H-2, 143-150	10.03	0.11		0.11	0.00
2H-5, 143-150	14.53	0.08		0.08	0.00
3H-2, 143-150	19.53	0.22		0.22	0.00
3H-5, 143-150	24.03	0.18	0.11	0.15	0.04
4H-2, 140-150	29.00	0.22		0.22	0.00
5H-2, 140-150	38.50	0.64	0.55	0.60	0.04
6H-2, 140-150	48.00	0.58	0.55	0.57	0.01
7H-2, 140-150	57.50	0.74	0.66	0.70	0.04
8H-2, 140-150	67.00				
9H-2, 140-150	76.50	0.55	0.67	0.61	0.06
10H-2, 140-150	86.00	0.65	0.61	0.63	0.02
11H-2, 140-150	95.50	0.51	0.41	0.46	0.05
12H-2, 140-150	105.00	0.63	0.48	0.56	0.08
13H-2, 140-150	114.50	0.42	0.47	0.45	0.03
14H-2, 140-150	124.00	0.41	0.37	0.39	0.02
15H-2, 140-150	133.50				
16H-2, 140-150	143.00	0.28	0.26	0.27	0.01
17H-2, 140-150	152.50	0.34	0.27	0.31	0.04
18H-2, 135-150	161.95	0.24	0.37	0.31	0.07
19H-2, 135-150	171.45	0.20	0.29	0.25	0.05
20H-2, 135-150	180.95	0.23	0.24	0.24	0.00
21H-2, 135-150	190.45	0.33	0.30	0.32	0.02
22H-2, 135-150	199.95	0.27	0.24	0.26	0.02
23H-2, 135-150	209.45	0.24	0.25	0.25	0.01
24H-2, 135-150	218.95	0.26	0.24	0.25	0.01
25H-2, 135-150	228.45	0.22	0.33	0.28	0.06
26H-2, 135-150	237.95	0.23		0.23	0.00
27H-2, 135-150	247.45	0.18	0.28	0.23	0.05
28H-2, 135-150	256.95	0.29	0.22	0.26	0.04
29H-2, 135-150	266.45	0.22	0.28	0.25	0.03
30X-2, 135-150	275.95	0.11	0.39	0.25	0.14
31X-2, 135-150	281.75				
32X-2, 135-150	287.55				
33X-2, 135-150	296.75				
34X-2, 135-150	305.95				
35X-2, 135-150	315.25				
38X-2, 135-150	342.65				
41X-2, 135-150	370.15				
44X-2, 135-150	397.55				
47X-2, 135-150	425.65				
50X-2, 135-150	452.95				
53X-2, 135-150	480.95				
56X-5, 135-150	512.75				
59X-2, 135-150	537.15				
62X-2, 135-150	566.05				
65X-2, 135-150	594.95				
68X-4, 135-150	626.85				
72X-5, 135-150	666.85				
75X-2, 135-150	691.25				
77X-2, 135-150	710.55				

Note: All samples were run in replicate, and values for individual analyses, means, and standard deviations (SD) are shown.

Table 5. The oxygen isotopic composition of samples from Site 1007.

Core, section, interval (cm)	Depth (m)	O #1	O #2	Mean	SD
166-1007B-					
1H-6, 145-150	5.95	0.43	0.44	0.44	0.00
2H-2, 140-150	8.98	0.35		0.35	
2H-4, 140-150	12.45	0.41	0.37	0.39	0.02
3H-2, 140-150	15.45	0.39	0.39	0.39	0.00
3H-4, 140-150	21.95	0.52		0.52	
4H-5, 140-150	24.95	0.42	0.54	0.48	0.06
5H-5, 140-150	35.45	0.51	0.68	0.60	0.09
6H-3, 140-150	47.45	1.08	1.06	1.07	0.01
7H-5, 140-150	53.95	1.20	1.19	1.20	0.00
8H-4, 135-150	64.95	1.21	1.34	1.28	0.07
9H-4, 140-150	72.93	1.33	1.31	1.32	0.01
10H-2, 140-150	82.45	1.37	1.30	1.34	0.04
11X-3, 140-150	87.65	1.31	1.35	1.33	0.02
15X-5, 140-150	96.15	1.39	1.37	1.38	0.01
16X-3, 135-150	128.05	1.46	1.45	1.46	0.00
17X-4, 135-150	142.93	1.56	1.55	1.56	0.00
18X-2, 0-15	153.33	1.48	1.45	1.47	0.01
23X-4, 135-150	158.38	1.61	1.54	1.58	0.04
24X-5, 135-150	209.03	1.79	1.93	1.86	0.07
25X-5, 135-150	219.83	1.99	1.96	1.98	0.01
26X-5, 135-150	228.93	1.96	1.95	1.96	0.00
27X-5, 135-150	238.03	2.10	2.08	2.09	0.01
28X-3, 135-150	247.23	2.13	2.08	2.11	0.03
29X-1, 135-150	253.43	2.18	2.04	2.11	0.07
30X-2, 135-150	259.43	2.22	2.12	2.17	0.05
32X-1, 135-150	270.63	2.09	2.05	2.07	0.02
38X-1, 0-1	287.43	2.34	2.19	2.27	0.07
166-1007C-					
6R-2, 0-10	341.16	2.37	2.34	2.36	0.01
12R-2, 123-135	351.55	2.25	2.26	2.26	0.00
14R-1, 112-122	410.49	2.47	2.50	2.49	0.01
15R-3, 83-94	428.17	2.39	2.36	2.38	0.02
17R-6, 99-114	440.59	2.43	2.53	2.48	0.05
19R-3, 134-145	464.47				
21R-2, 130-142	479.60	2.48	2.41	2.45	0.03
24R-5, 136-144	497.26				
26R-6, 105-121	530.70				
28R-3, 103-116	551.13	2.32	2.51	2.42	0.10
31R-6, 105-121	575.50				
34R-1, 135-152	599.23	2.45	2.35	2.40	0.05
37R-1, 0-12	620.84	2.44	2.40	2.42	0.02
40R-4, 139-150	648.36	2.17	2.21	2.19	0.02
43R-2, 79-92	683.05				
45R-2, 0-12	708.36	2.39	2.37	2.38	0.01
47R-2, 0-14	726.99				
49R-2, 112-124	746.21				
52R-2, 31-44	765.68				
54R-3, 9-16	794.48				
57R-2, 0-10	815.03				
60R-1, 98-113	842.25				
62R-2, 0-13	870.56				
66R-2, 28-39	890.27				

Note: All samples were run in replicate, and values for individual analyses, means, and standard deviations (SD) are shown.

orated seawater that has become entrapped in rocks during sea-level low stands. However, the evaporated seawater origin is not supported by absence of a correlation between $\delta^{18}O$ and δD. Therefore, the origin of the increase in salinity is still an enigma: whereas the absence of a correlation between $\delta^{18}O$ and δD (Fig. 11) suggests the dissolution of NaCl, the absence of a change in the Na/Cl ratio with increasing depth tends to favor the presence of a deep-seated saline fluid.

Carbonate Diagenesis

Typically, pore waters in deep-sea sediments show a decrease in their $\delta^{18}O$ values as a result of the interaction between pore water and igneous basement rocks (Lawrence, 1989). In the Bahamas, because the influence of interactions with basement rocks is likely to be minimal at the depths drilled in this study, the observed increase in $\delta^{18}O$ at most sites is best explained as a result of the recrystallization of biogenic carbonate components in the presence of a geothermal gradient. The magnitude of the expected changes resulting from recrystallization of carbonates will depend upon the amount of recrystallization, the geothermal gradient, and the $\delta^{18}O$ of the initial sediment and pore water. Using the equations presented by previous researchers (Lawrence, 1973, 1989; Lawrence et al., 1976; Killingley, 1983; Stout, 1985), the isotopic composition of the pore water after a specified amount of recrystallization can be calculated from the following equation:

$$\delta w_e = \frac{M_c R[\delta C_i + 10^3(1 - \alpha_T)] + M_w \delta w_i}{M_w + M_c \alpha_T R} \quad (1)$$

In this equation:

δw_e = $\delta^{18}O$ of interstitial water after recrystallization,
δC_i = $\delta^{18}O$ of calcium carbonate of initial sediment,
δw_i = $\delta^{18}O$ of interstitial waters before reaction,
M_c = mole fraction of oxygen in carbonate sediment,
M_w = mole fraction of oxygen in pore waters,
R = percentage of recrystallization, and
α = fractionation factor between calcite-water.

As an example, Figure 12 shows the evolution of the interstitial water (δw_e) in the presence of various different conditions that are

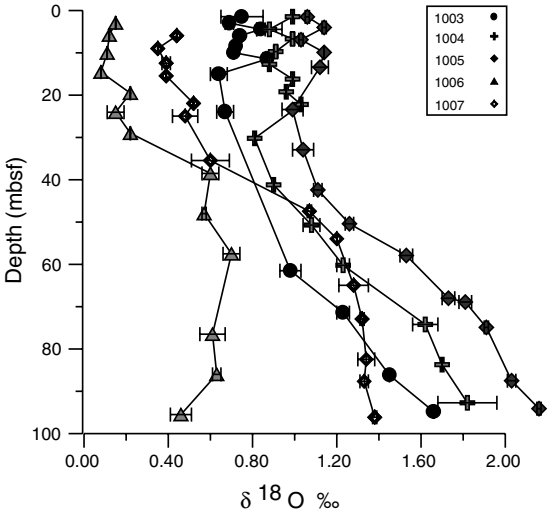

Figure 6. Variations in the $\delta^{18}O$ of the pore waters from the upper 100 mbsf, Sites 1003–1007. Note the decrease in the $\delta^{18}O$ of the pore fluids at Sites 1004 and 1005 corresponding to the decrease seen in the Cl^-. Error bars represent ±1 standard deviation.

Table 6. Mean $\delta^{18}O$ and chloride concentrations over the upper 30 m of sediment.

Sites	$\delta^{18}O$ (‰)	SD	Cl^- (mM)	SD
1005	+1.07	0.05	581	2.2
1004	+0.94	0.07	572	5.6
1003	+0.74	0.07	576	1.8
1007	+0.45	0.08	566	7.5
1006	+0.15	0.05	564	2.6

Note: SD = standard deviation.

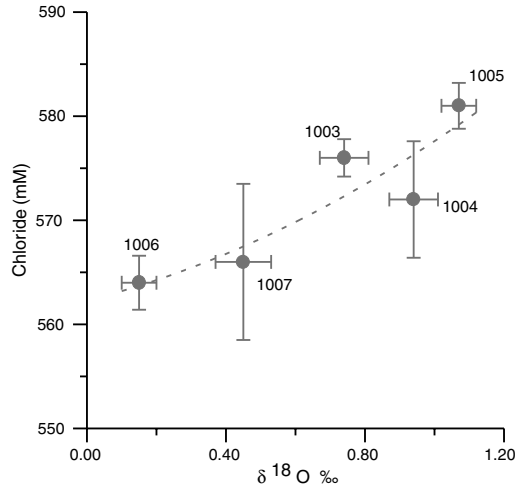

Figure 7. Mean chloride concentrations and $\delta^{18}O$ values for the upper 30 mbsf, Sites 1003–1007. Note the decrease in the $\delta^{18}O$ as the sites become farther from the platform margin. Chloride data are from Eberli, Swart, Malone, et al. (1997). Error bars represent ±1 standard deviation of the mean of the values in the upper 30 mbsf.

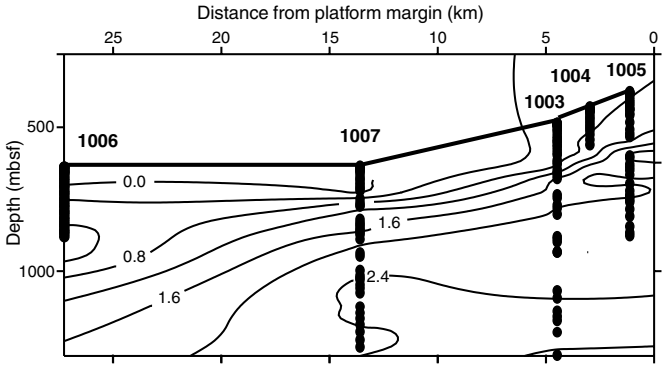

Figure 8. Contour map of the oxygen isotopic composition of the pore waters shown in meters below seafloor, Sites 1003–1007. Sites 1005 is located on the right side of the figure and is closest to the platform margin, whereas Site 1006 is located 25 km from the margin. The heavy $\delta^{18}O$ values close to the platform reflect the increasing amount of carbonate diagenesis taking place in this region.

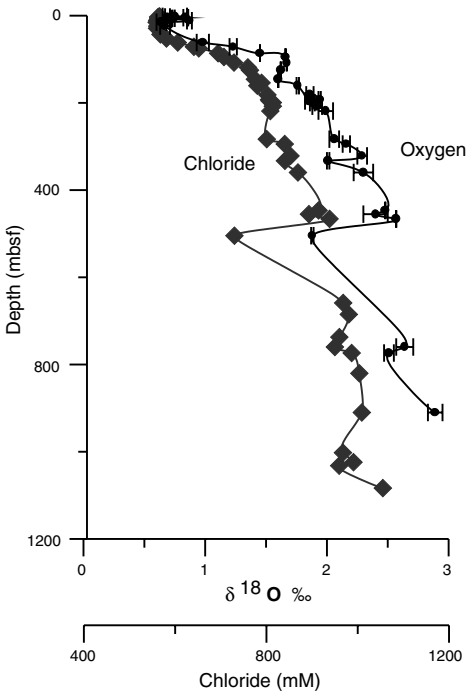

Figure 9. Oxygen and chloride profile vs. depth, Site 1003. Note the covariance between $\delta^{18}O$ and Cl^-. Error bars represent ±1 standard deviation.

likely to occur during burial. Case A represents a geothermal gradient of 50°C/km, an initial sediment $\delta^{18}O$ value of +0.0‰ Peedee belemnite (PDB), an initial water $\delta^{18}O$ value of 0.5‰ SMOW, and a recrystallization rate of 1% per 5 m. Case B represents the same conditions with the exception of a geothermal gradient of 70°C/km. Case C represents the same conditions as Case A except that the initial oxygen isotopic composition of the water is +0.5‰. In all cases shown in Figure 12, the $\delta^{18}O$ increases to values consistent with those observed at the Leg 166 sites.

The only exception to the trend of increasing pore-water $\delta^{18}O$ with increasing depth was seen at Site 1006 (Fig. 10). The absence of an increase in $\delta^{18}O$ at this site is probably a consequence of reduced amounts of carbonate diagenesis compared to the other more proximal locations (Eberli, Swart, Malone, et al., 1997; Shipboard

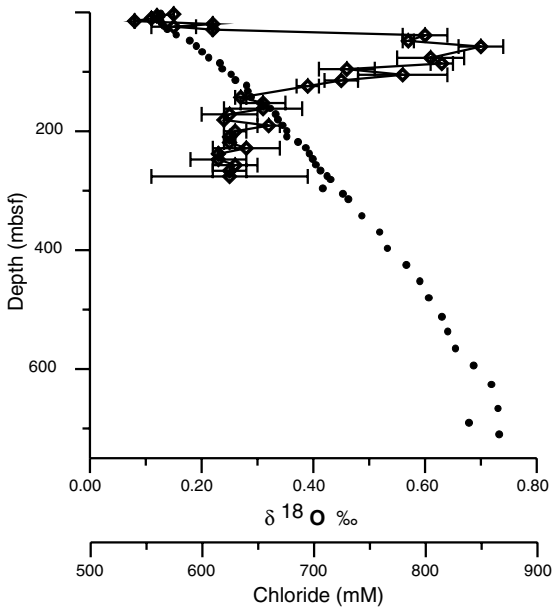

Figure 10. Oxygen (dots) and chloride (diamonds) profile, Site 1006. Note the absence of covariance between $\delta^{18}O$ and Cl^-. Error bars represent ±1 standard deviation.

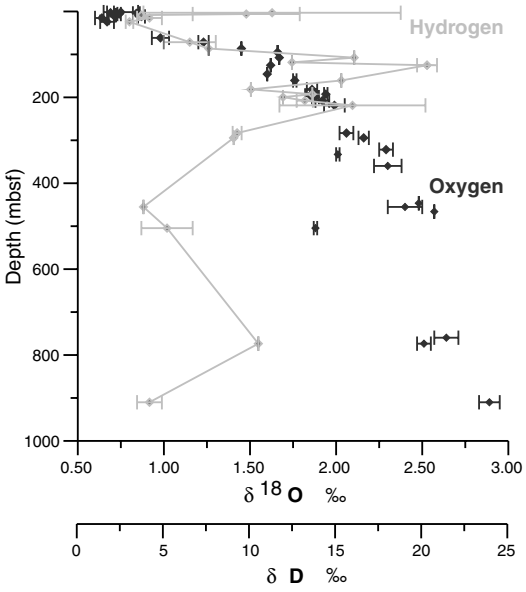

Figure 11. Oxygen and hydrogen isotopic profile, Site 1003. The δD is decoupled from the change in $\delta^{18}O$, indicating that $\delta^{18}O$ is controlled by carbonate recrystallization reactions. Error bars represent ±1 standard deviation.

Scientific Party, 1997). The relative absence of carbonate diagenesis is evident from the excellent preservation of the foraminifers and nannofossils, which made this site a particularly good one for biostratigraphic purposes (Shipboard Scientific Party, 1997).

Water Movement into the Platform

Some support for water being drawn into the platform was provided by unusual chloride profiles, particularly at Sites 1004 and 1005 (Fig. 3). These profiles suggested that less-saline bottom water was being drawn into the platform, perhaps by a mechanism such as Kohout convection (Kohout, 1966; Simms, 1984). An alternative scenario is that more-saline water, originating from the platform top, is sinking downward through the upper sediments. Although the anomaly in the chloride was also present as slightly depressed $\delta^{18}O$ values, the data are consistent with either explanation for the origin of the Cl^- anomaly.

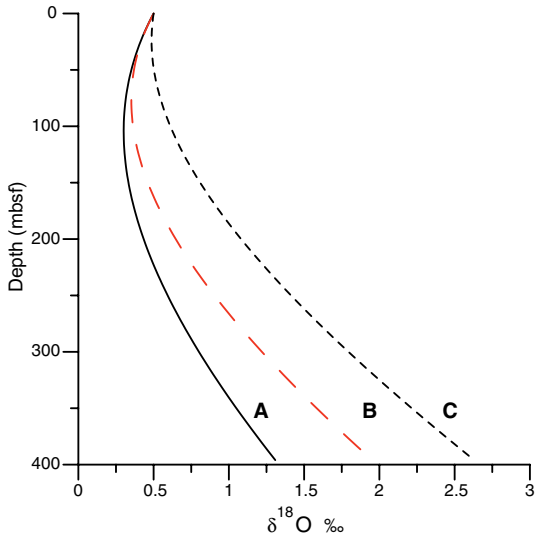

Figure 12. Model pore-water results using Equation 1. Case A represents a geothermal gradient of 50°C/km, an initial sediment $\delta^{18}O$ value of +0.0‰ PDB, an initial water $\delta^{18}O$ value of 0.5‰ SMOW, and a recrystallization rate of 1% per 5 m. Case B represents the same conditions with the exception of a geothermal gradient of 70°C/km. Case C represents the same conditions as Case A, except that the initial oxygen isotopic composition of the water is +0.5 ‰.

CONCLUSIONS

Several conclusions may be drawn from this study. First, the absence of a gradient in the $\delta^{18}O$ in the upper portion of Sites 1003 through 1007 is consistent with the idea that advection of water through this region is removing the geochemical gradients normally produced by diffusion and carbonate diagenesis. However, we cannot rule out the possibility that the observed geochemical patterns are a result of high rates of sedimentation in the upper portion of the profile.

Second, increases in $\delta^{18}O$ of the pore water with depth are not traceable to diffusion from an underlying source high in $\delta^{18}O$ but result principally from recrystallization of existing metastable carbonate sediments to low-Mg calcite and dolomite. The increases in $\delta^{18}O$ of the pore waters are most prominent in the sites closest to the platform and are reduced at Site 1006, reflecting higher rates of carbonate recrystallization closer to the platform.

Third, pore waters throughout the flushed zone show elevated $\delta^{18}O$ values at the sites closest to the platform, suggesting the fluids from the platform top are influencing the salinity of bottom waters.

ACKNOWLEDGMENTS

The author would like to thank Phil Kramer and Eric de Carlo for their help in processing the samples. Amel Saied is acknowledged for her assistance in the laboratory. Finally, the high precision of the oxygen isotopic values would not have been possible without the assistance of Europa Scientific, and especially Simon Prosser.

REFERENCES

Austin, J.A., Jr., Schlager, W., et al., 1986. *Proc. ODP, Init. Repts.,* 101: College Station, TX (Ocean Drilling Program).

Coplen, T.B., Wildman, J.D., and Chen, J., 1991. Improvements in the gaseous hydrogen-water equilibration technique for hydrogen isotope ratio analysis. *Anal. Chem.,* 63:910–912.

Baker, P.A., Gieskes, J.M., and Elderfield, H., 1982. Diagenesis of carbonates in deep-sea sediments: evidence from Sr^{2+}/Ca^{2+} ratios and interstitial dissolved Sr^{2+} data. *J. Sediment. Petrol.,* 52:71–82.

Eberli, G.P., Swart, P.K., Malone, M.J., et al., 1997. *Proc. ODP, Init. Repts.,* 166: College Station, TX (Ocean Drilling Program).

Epstein, S., and Mayeda, T., 1953. Variation of ^{18}O content of waters from natural sources. *Geochim. Cosmochim. Acta,* 4:213–224.

Friedman, I., 1957. Deuterium content of natural water and other substances. *Geochim. Cosmochim. Acta,* 4:89–103.

Gieskes, J.M., 1973. Interstitial water studies, Leg 15: alkalinity, pH, Mg, Ca, Si, PO_4, and NH_4. *In* Heezen, B.C., MacGregor, I.D., et al., *Init. Repts. DSDP,* 20: Washington (U.S. Govt. Printing Office), 813–829.

————, 1974. Interstitial water studies, Leg 25. *In* Simpson, E.S.W., Schlich, R., et al., *Init. Repts. DSDP,* 25: Washington (U.S. Govt. Printing Office), 361–394.

Killingley, J.S., 1983. Effects of diagenetic recrystallization on $^{18}O/^{16}O$ values of deep-sea sediments. *Nature,* 301:594–597.

Kohout, F.A., 1966. Submarine springs: a neglected phenomenon of coastal hydrology. *Central Treaty Org. Symp. Hydrol. Water Res. Dev.,* 391–413.

Lawrence, J.R., 1973. Interstitial water studies, Leg 15—stable oxygen and carbon isotope variations in water, carbonates, and silicates from the Venezuela Basin (Site 149) and the Aves Rise (Site 148). *In* Heezen, B.C., MacGregor, I.D., et al., *Init. Repts. DSDP,* 20: Washington (U.S. Govt. Printing Office), 891–899.

————, 1989. The stable isotope geochemistry of deep-sea pore water. *In* Fritz, P., and Fontes, J.C. (Eds.), *Handbook of Environmental Isotope Geochemistry* (Vol. 3) (2nd ed): Amsterdam (Elsevier), 317–356.

Lawrence, J.R., Gieskes, J., and Anderson, T.F., 1976. Oxygen isotope material balance calculations, Leg 35. *In* Hollister, C.D., Craddock, C., et al., *Init. Repts. DSDP,* 35: Washington (U.S. Govt. Printing Office), 507–512.

Manheim, F.T., and Sayles, F.L., 1974. Composition and origin of interstitial waters of marine sediments, based on deep sea drill cores. *In* Goldberg, E.D. (Ed.), *The Sea* (Vol. 5): *Marine Chemistry: The Sedimentary Cycle:* New York (Wiley), 527–568.

Shipboard Scientific Party, 1997. Leg synthesis: sea-level changes and fluid flow on the Great Bahama Bank slope. *In* Eberli, G.P., Swart, P.K., Malone, M.J., et al., *Proc. ODP, Init. Repts.,* 166: College Station, TX (Ocean Drilling Program), 13–22.

Simms, M., 1984. Dolomitization by groundwater-flow systems in carbonate platforms. *Trans. Gulf Coast Assoc. Geol. Soc.,* 34:411–420.

Stout, P.M., 1985. Chemical diagenesis of pelagic biogenic sediments from the Equatorial Pacific [Ph.D. dissertation]. Univ. of Calif., San Diego.

Swart, P.K., and Guzikowski, M., 1988. Interstitial-water chemistry and diagenesis of periplatform sediments from the Bahamas, ODP Leg 101. *In* Austin, J.A., Jr., Schlager, W., et al., *Proc. ODP, Sci. Results,* 101: College Station, TX (Ocean Drilling Program), 363–380.

Date of initial receipt: 13 August 1998
Date of acceptance: 6 April 1999
Ms 166SR-130